Salmonella immunotherapy engineered with highly efficient tumor antigen coating establishes antigen-specific CD8+ T cell immunity and increases in antitumor efficacy with type I interferon combination therapy

Suyang Wang, Michelle Cheng, Chao-Cheng Chen, Chia-Yu Chang, Ya-Chea Tsai, Jr-Ming Yang, TC Wu, Chuan-Hsiang Huang & Chien-Fu Hung

View supplementary material

Published online: 27 Dec 2023.

Submit your article to this journal

Article views: 43

View related articles

View Crossmark data

Taylor & Francis
Taylor & Francis Group

ORIGINAL RESEARCH

🔓 OPEN ACCESS | Check for updates

Salmonella immunotherapy engineered with highly efficient tumor antigen coating establishes antigen-specific CD8+ T cell immunity and increases in antitumor efficacy with type I interferon combination therapy

Suyang Wang[a], Michelle Cheng[a], Chao-Cheng Chen[a], Chia-Yu Chang[a], Ya-Chea Tsai[a], Jr-Ming Yang[a], TC Wu[a,b,c,d], Chuan-Hsiang Huang[a], and Chien-Fu Hung[a,b]

[a]Department of Pathology, Johns Hopkins University School of Medicine, Baltimore, MD, USA; [b]Department of Oncology, Johns Hopkins University School of Medicine, Baltimore, MD, USA; [c]Department of Obstetrics and Gynecology, Johns Hopkins University School of Medicine, Baltimore, MD, USA; [d]Molecular Microbiology and Immunology, Johns Hopkins University School of Medicine, Baltimore, MD, USA

ABSTRACT

Bacteria-based cancer therapy employs various strategies to combat tumors, one of which is delivering tumor-associated antigen (TAA) to generate specific immunity. Here, we utilized a poly-arginine extended HPV E7 antigen (9RE7) for attachment on Salmonella SL7207 outer membrane to synthesize the bacterial vaccine Salmonella-9RE7 (Sal-9RE7), which yielded a significant improvement in the amount of antigen presentation compared to the previous lysine-extended antigen coating strategy. In TC-1 tumor mouse models, Sal-9RE7 monotherapy decreased tumor growth by inducing E7 antigen-specific immunity. In addition, pairing Sal-9RE7 with adjuvant Albumin-IFNβ (Alb-IFNβ), a protein cytokine fusion, the combination significantly increased the antitumor efficacy and enhanced immunogenicity in the tumor microenvironment (TME). Our study made a significant contribution to personalized bacterial immunotherapy via TAA delivery and demonstrated the advantage of combination therapy.

Introduction

With improvements in genetic engineering techniques, bacteria-based cancer therapies have gained increasing attention as a versatile complement to conventional treatment strategies.[1,2] Recent discoveries have shed light on their cancer therapeutic characteristics, including specific targeting hypoxic tumor microenvironment (TME) by anaerobic strains, immunostimulatory action on professional antigen-presenting cells (APCs) and cascade responses, and diverse modifications for improved antitumor activities.[3–7] Among these therapeutic bacterial species, *Salmonella* (S. typhimurium) is one of the most well-researched and promising candidates, due to its superior tumor targeting and growth suppression abilities.[8] Improvements on bacterial target specificity and virulence attenuation has allowed growing engineering innovation of cytotoxin and immune cytokine delivery by bacteria to the TME.[9,10] One direction of *Salmonella*-based cancer immunotherapy is generating tumor-specific immunity through the delivery of immune dominant tumor antigen.[11] A previous study presented an antigen-coated bacterial platform using cell penetrating peptide (CPP) linkage to induce antigen-specific immunity, but it showed limited tumor reduction as a lone treatment strategy.[12] After combining the bacterial vaccine with immune checkpoint inhibitor (ICI) therapy, it improved the response rate and efficacy of the ICI treatment.[12]

Nowadays, many cancer therapies utilize combination treatments to avoid cancer resistance by targeting multiple mechanisms.[13] As a well-established target for viral infections and cancer, type I interferons, a major class of immune cytokines, can act directly on CD8+ T cells to increase cytotoxicity and survival by increasing the expression of cytotoxic T cell markers, perforin 1 and granzyme B115.[14,15] It has also been reported to inactivate suppressiveness of regulatory T cells (Treg) to promote effector functions.[16] In clinical settings, type I interferon has been used for resected stage II and III melanoma, and it could increase the rate of molecular responses in chronic myeloid leukemia when combined with multikinase inhibitor imatinib.[17–19] Recently, we have improved on the drug kinetics and functionality of a type I interferon, interferon beta (IFNβ), by fusing it to albumin protein, creating Albumin-IFNβ (Alb-IFNβ).[20] This increases the half-life of IFNβ, and therefore enhanced cross-presentation by APCs and generated stronger antigen-specific T cell and B cell responses.

Based on the bacterial immunotherapy strategy of tumor antigen delivery, we have developed a *Salmonella*-based cancer vaccine to induce E7 antigen-specific immunity. Extending HPV E7 antigen by 9 cationic arginine residues (9RE7), this modified antigen peptide can adhere to the cell membrane of *Salmonella* Typhimurium strain SL7207,[10] termed Sal-9RE7. Poly-l-arginine is used as a tag for mammalian cell uptake to deliver drugs and macromolecules such as proteins and enzymes.[21] By generating E7-specific CD8+ T cells and recruiting CD4+ helper T cells to the

TME, Sal-9RE7 exhibited promising antitumor effects as a monotherapy. When combined with protein adjuvant Alb-IFNβ, the antitumor effect was significantly enhanced with increased antigen-specific cytotoxic T Lymphocytes (CTLs) proliferation and decreased exhaustion and suppression of tumor infiltrating lymphocytes (TILs). Our results demonstrated the therapeutic efficacy of an HPV E7 antigen-presenting *Salmonella* system with improved peptide loading and should be considered for future bacterial immunotherapy approaches in clinical investigations.

Materials and methods

Cells and bacteria

E7 expressing TC-1 tumor cells and dendritic cell lines[22,23] were grown in vitro in RPMI 1640 media containing 10% (v/v) fetal bovine serum, 50 units/mL of penicillin/streptomycin, 2 mM L-glutamine, 1 mM sodium pyruvate, 2 mM non-essential amino acids, and 0.1% (v/v) 2-mercaptoethanol under 37°C with 5% CO_2. CD8+ T cells were incubated with E7 expressing cells and maintained in culture. *Salmonella* SL7207 was grown under the recommended conditions in LB broth at 37°C. Cells were harvested at O. D. 600 reading of 0.5 and washed with PBS solution before incubation at 60°C for 2 hours. Bacterial activity was checked by growing in LB medium at 37°C with no O.D. 600 reading to ensure complete inactivation.

Peptide synthesis

Peptides used in this study include RRRRRRRRR-RAHYNIVTF (E7 protein amino acids 49–57), termed 9RE7, and FITC-conjugated peptides KKKKKK (6K), RRRRRR (6 R), RRRRRRRRR (9 R), E7, and 9RE7. Peptides were synthesized by GenScript (Piscataway, NJ, USA).

Characterization of Sal-9RE7

5×10^6 CFU of live or heat inactivated *Salmonella* SL7207 was mixed with 1ug of FITC conjugated peptides 6K, 6 R, 9 R, E7, and 9RE7 in PBS buffer. Bacteria/peptide mixture was vortexed at room temperature for 30 minutes, followed by centrifugation and buffer exchange to remove unbound peptides. FITC signals were measured by 13-color B-Y-R-V CytoFLEX S (Beckman Coulter). Bacterial cell charge was measured with Malvern Zetasizer Nano ZS90 (Malvern Instruments). 9RE7 attachment was quantified by interpolating the absorbance of FITC-labeled Sal-9RE7 at 500 nm from the constructed standard curve with Nanodrop One (Thermo Fisher Scientific).

Alb-IFNβ protein generation

Generation of mouse pcDNA3-Alb-IFNβ Mouse IFNβ plasmid was performed as previously described.[20] We transfected Alb-IFNβ plasmid in Expi293F expression system kit (Thermo Fisher Scientific) and purified the proteins by the HiTrap Albumin column (GE Healthcare Life Sciences).

In vitro T cell activation

Sal-9RE7 was constructed by mixing 1×10^8 CFU of heat-inactivated *Salmonella* to 1 ug 9RE7 and incubated with 1×10^5 dendritic cells in 96 well plate cultured with complete RPMI media at 37°C, 5% CO2 overnight. After aspirating culture medium and washing with PBS, 5×10^5 E7-specific CD8+ T cells were added to dendritic cell line and blocked with Brefeldin A + Monensin Golgi Plug (Thermo Fisher Scientific) overnight.[22,23] Cells were collected and stained with PE-conjugated HPV16 E7aa49–57 peptide loaded H-2 Db E7 tetramer and APC-A750-conjugated anti-mouse CD8α antibody (Biolegend) before permeabilization with eBioscience Fixation (Invitrogen). FITC-conjugated IFNγ antibody was used for intracellular staining.[24]

Mice

Female C57BL/6 mice aged 6–8 weeks were purchased from Charles Rivers Laboratories (Frederick, Maryland, USA), and housed under specific pathogen-free conditions at the Johns Hopkins University School of Medicine Animal Facility (Baltimore, Maryland, USA). All animal procedures were performed according to protocols approved by the Johns Hopkins Institutional Animal Care and Use Committee. Recommendations for the proper use and care of laboratory animals were closely followed.

Mice vaccination

For tumor inoculation, 1×10^5 TC-1 cells in 50 μL of PBS were subcutaneously injected into 6–8 weeks old female C57BL/6 mice at the lower right abdomen. Largest length and width were measured by digital calipers twice per week. Tumor volumes were calculated by the formula: $V = (Length \times Width^2)/2$. At the indicated time points, TC-1 tumor-bearing mice were vaccinated with 10 ug of 9RE7 peptides, 10^8 CFU of heat inactivated *Salmonella*, Sal-9RE7 (10^8 CFU to 10 ug), 50 ug of Alb-IFNβ, or Alb-IFNβ combined with Sal-9RE7. 9RE7 peptide and Alb-IFNβ were delivered intraperitoneally, and bacteria were injected subcutaneously at the tumor side of the abdomen.

Flow cytometry analyses

Peripheral Blood Mononuclear Cells (PBMC) from blood samples were collected by red blood cell (RBC) lysis using RBC lysis buffer (eBioscience). For intratumoral immune cell preparation, tissue was collected from mice into FACS buffer with magnesium and calcium. After mincing with scissors into ~2 mm pieces, tissue digestion enzymes including Collagenase I, Collagenase IV, and DNase I were added to samples and incubated for 20 minutes at 37 degree Celsius. After centrifugation and extensive washing, tumor samples were purified by loading onto Ficoll-Paque Plus (GE Healthcare Life Sciences, Marlborough, MA). Tubes were centrifuged for 20 minutes with low acceleration and no brake. Ficoll-RPMI interface was collected. Samples were then counted, plated at equal cell numbers, and prepared for flow cytometry. Prior to antibody

staining, Zombie Aqua live/dead (BioLegend) and Fc Block were used to identify dead cells and reduce nonspecific antibody binding. Antigen-specific CD8+ T cell population in PBMC was identified with PE-conjugated E7 tetramer and APC-A750-conjugated anti-mouse CD8α antibodies. For tumor infiltrating lymphocyte analyses, we used PE-Cy5-conjugated anti-mouse CD45 antibodies, BV421-conjugated anti-mouse CD3 antibodies, PE-conjugated anti-mouse CD8 antibodies, BV780-conjugated anti-mouse CD4 antibodies, APC-A750 conjugated anti-mouse PD-1 antibodies, PE-Cy7-conjugated anti-mouse CD25 antibodies, and APC-conjugated FoxP3 antibodies. Fluorescent compensation was generated using single-antibody controls on the CytExpert 2.0 software (Beckman). FACS analysis was performed using CytoFLEX S (Beckman) and data were analyzed by FlowJo software.

Statistical analysis

All data statistical analysis was performed with GraphPad Prism V.10 software and represented as means and standard error of the mean. Kaplan-Meier survival plots were used to estimate the survival percentage and tumor-free rate. Long rank tests were used to compare the survival time between treatment groups. Comparison between individual data points were analyzed for variance with one-way ANOVA and the Tukey – Kramer multiple comparison test, $^*p \leq 0.05$, $^{**}p \leq 0.01$, $^{***} p \leq 0.001$, $^{****} p \leq 0.0001$, ns=not significant.

Results

Poly-arginine-tagged HPV E7 antigen effectively attaches to heat inactivated Salmonella

To improve on the previous PolyK anchored antigen model[12], we used cell penetrating peptide poly-arginine as the attachment moiety of 9RE7. We were able to determine an optimal binding condition by comparing live attenuated or 60°C heat inactivated Salmonella (5×10^6 CFU to 1ug peptide) incubated with FITC-conjugated 9RE7. The amount of FITC-conjugated 9RE7 on Salmonella were quantified with nanoscale flow cytometry (Figure 1a) that showed the significantly higher FITC intensity under heat-inactivated conditions. Hence, all subsequent experiments used heat-inactivated Salmonella to maximize capturing of the 9RE7 peptide in Sal-9RE7. Next, we compared the binding strength of various FITC-labeled cationic peptides including PolyK hexamer (6K-FITC), PolyR hexamer (6 R-FITC), and PolyR nonamer (9 R-FITC) to Salmonella. Among these peptides, 9 R-FITC showed the largest shift in nanoscale flow cytometry (Figure 1b,c), thus binding significantly more units of peptide than the previous PolyK strategy. With the added 9 R moiety, 9RE7 showed significantly higher affinity to Salmonella than E7 alone (Figure 1d,e). By enriching Salmonella with 9RE7, the cell membrane charge was altered as measured by their zeta potential (Figure 1f), imparting arginine's positive charge on the neutral
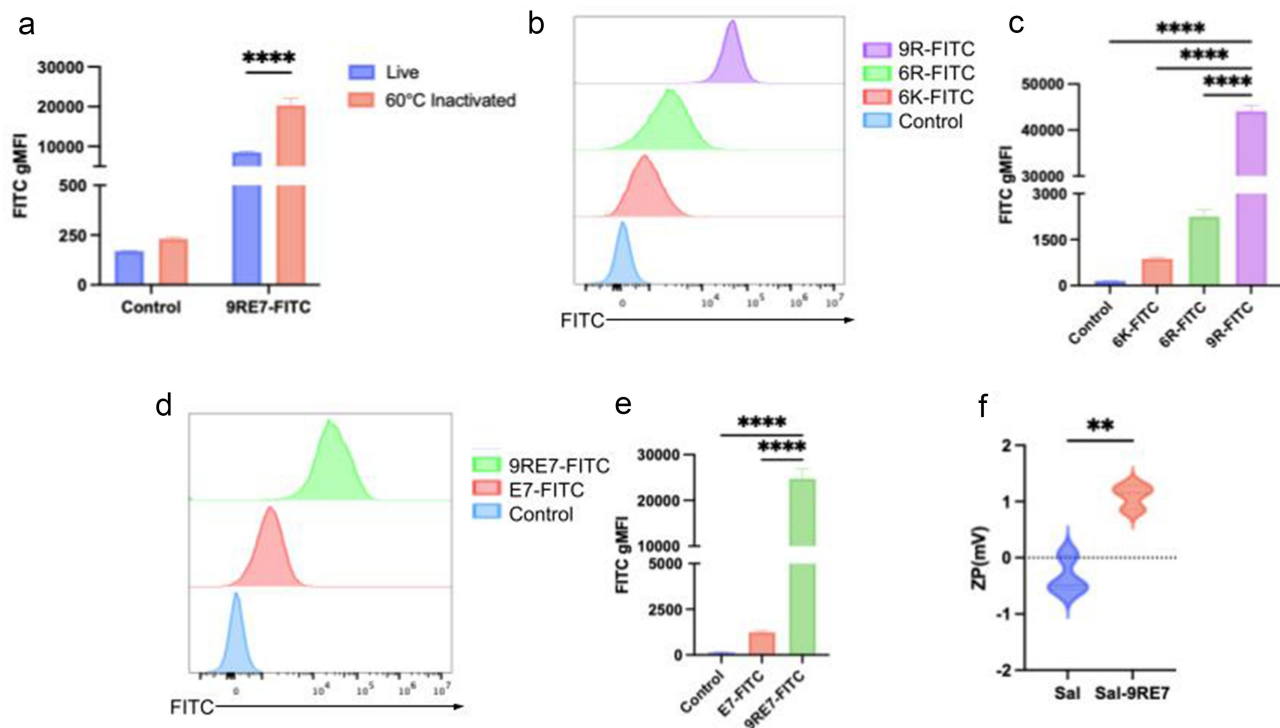

Figure 1. Characterization of Salmonella's electrostatic binding affinity to poly-arginine extended E7 antigen. (a) Nanoscale flow cytometry analysis of FITC signal of live and 60°C heat-inactivated Salmonella (5×10^6 CFU) binding with 1 ug of FITC-conjugated HPV E7 antigen extended by 9 arginine residues (9RE7-FITC). Heat inactivated Salmonella conjugates with 1 ug of FITC conjugated poly-lysine hexamer (6K-FITC), poly-arginine hexamer (6R-FITC), or poly-arginine nonamer (9R-FITC) with (b) representative flow cytometry histogram and (c) bar graph to compare polypeptide anchor strength. (d) Flow cytometry analysis of heat inactivated Salmonella binding strength with either FITC-labeled E7 or 9RE7 antigen peptide, and (e) bar graph representation. (f) Dynamic light scattering analysis comparing heat inactivated Salmonella (sal) before and after binding to 10ug of 9RE7 (Sal-9RE7). Performed with one-way ANOVA test *p<0.05, **p<0.01, ****p<0.0001. FITC, fluoresceinisothiocyanate.

bacterial membrane. To quantify 9RE7 attachment efficiency, we characterized the absorbance of FITC-conjugated 9RE7 UV-Vis spectrum at 500 nm (**Supplementary Figure S1A**). Through construction of the calibration standard curve (**Supplementary Figure S1B**), we calculated that 96.5% of 9RE7-FITC remained attached to *Salmonella* surface after buffer exchange.

Dendritic cells cross-present E7 antigen from Sal-9RE7 to activate antigen-specific CD8+ T cell response

Next, we sought to demonstrate Sal-9RE7 as an adjuvant to activate dendritic cells, which would cross-present tumor antigen to activate E7-specific CD8+ T cells. FITC-labeled Sal-9RE7 was prepared to coculture with dendritic cells to illustrate proper uptake by professional APCs. Upon removal of residual bacteria in culture medium, FITC labeled Sal-9RE7 cocultured dendritic cells showed elevated FITC signal through flow cytometry (Figure 2a,b), thus proving dendritic cells successfully phagocytized the bacterial complex. To show dendritic cell cross-presentation through major histocompatibility complex (MHC) class I, we treated dendritic cells with Sal-9RE7 before coculturing with E7-specific CD8+ T cell. The Sal-9RE7 treated group showed the highest IFNγ expression by E7+ CD8+ T cells, whereas inactivated *Salmonella* alone could not induce T cell activation (Figure 2c,d). Our results indicated that in an *in vitro* setting, Sal-9RE7 can effectively re-activate E7-specific CD8+ T cell via MHC class I presentation by APCs.

Administration of Sal-9RE7 in vivo shows significant antigen-specific CD8+ T cell immunity and antitumor efficacy

To assess the viability of Sal-9RE7 as an immunogenic vaccine and promote CTL-mediated antitumor response, we treated C57BL/6 mice bearing E7-positive TC-1 tumors with heat inactivated *Salmonella*, 9RE7 antigen peptide, or Sal-9RE7 for three times at one-week intervals (Figure 3a). While *Salmonella* or 9RE7 alone showed no effect on tumor growth, treatment with Sal-9RE7 yielded the smallest average tumor volume at the 30-day time point (Figure 3b). Accordingly, Sal-9RE7 treated tumor bearing mice survived longer than other groups (Figure 3c). One week after the third dose, we examined PBMC from all groups to compare E7 antigen-specific CD8+ T cell expansion. Reflecting the antitumor results, flow cytometry analysis showed generation of significantly higher E7+ CD8+ CTL population under Sal-9RE7 treatment (Figure 3d, e). Tumor antigen 9RE7 alone was insufficient to induce antigen-specific immunity without *Salmonella* as the adjuvant. These results proved that Sal-9RE7 can induce potent E7-specific CD8+ T cell mediated response *in vivo*, while simultaneously suppressing tumor growth and prolonging survival.

Coadministration of albumin-fused IFNβ cytokine and sal-9RE7 can improve on tumor treatment and antigen-specific CD8+ T cell responses

Due to Alb-IFNβ's prominent effect on expanding antigen-specific CD8+ T cells,[20] we believed it would act as a powerful adjuvant to enhance CD8+ T cell mediated immunity induced by Sal-9RE7 treatment. When coadministering
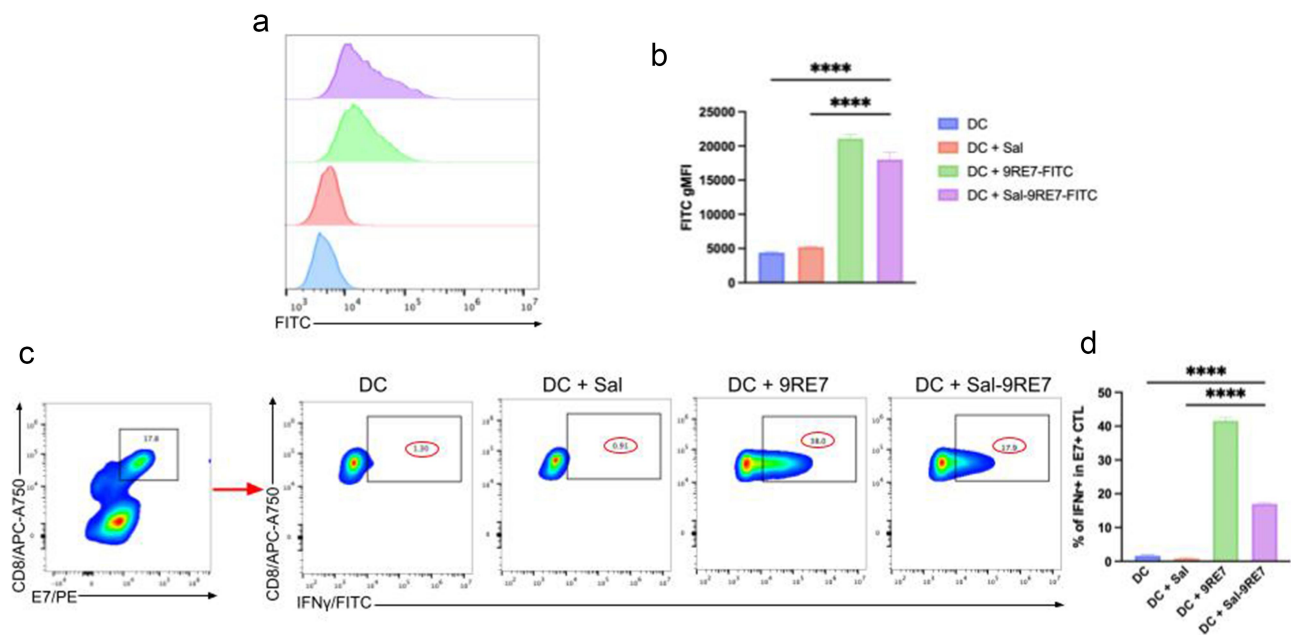

Figure 2. In vitro sal-9RE7 uptake by dendritic cell and T cell activation analysis. (a) Overnight dendritic cell line coincubation with 1×10^8 CFU of sal mixed with 1ug of 9RE7-FITC (Sal-9RE7-FITC), 9RE7-FITC, or sal is analyzed by flow cytometry histogram and (b) bar graph comparison of FITC geometric MFI in dendritic cells. (c) Flow cytometry analysis of E7-specific T cell activation. Sal, 9RE7, or Sal-9RE7 is added to dendritic cells before coculturing with E7-specific T cells in RPMI for another 24 hrs. After collecting the coculture mixture, cells are stained with PE-conjugated HPV16 E7aa49–57 peptide-loaded H-2 Db E7 tetramer and APC-A750-conjugated anti-mouse CD8α antibodies before cell membrane permeation and FITC anti-mouse IFNγ antibody for flow cytometry analyses. Representative flow cytometric images show E7 and CD8α gating strategy first, then positive population is gated for IFNγ. (d) Bar graph summary of E7 positive T cells with positive IFNγ population. ****p<0.0001.
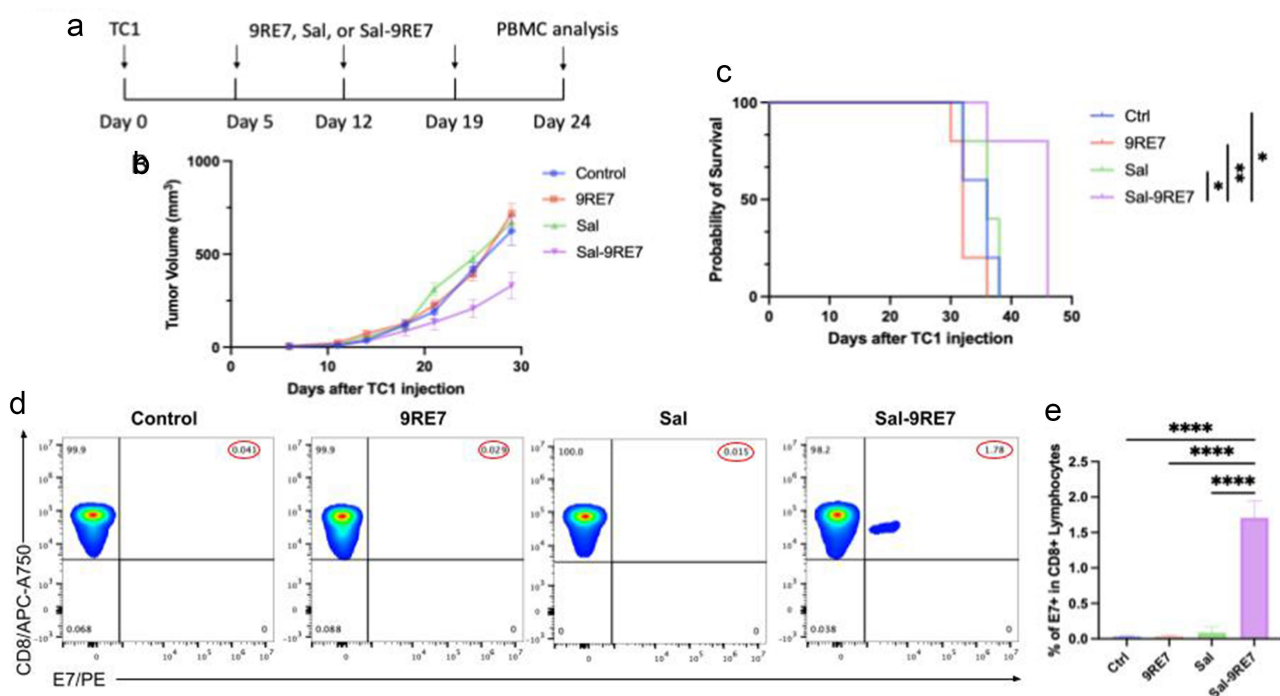
Figure 3. Characterization of therapeutic antitumor effect and antigen-specific CD8+ T cell immune response in TC1 tumor bearing mice treated with Sal-9RE7. (a) Schematic illustration of experiment schedule. C57BL/6 mice are injected with 1×10^5 TC-1 cells S.C. On day 0. They are given weekly treatments of either 10ug 9RE7 intraperitoneally, 1×10^8 heat inactivated *Salmonella* S.C., or Sal-9RE7 (1×10^8 CFU bacteria mixed with 10 ug of peptide) S.C. For 3 weeks. (b) Tumor growth curve of TC-1 tumor-bearing mice. (c) Kaplan-Meier survival curve of TC-1 tumor-bearing mice. (d) PBMC is collected from the mice one week after the final treatment for E7-specific T cell analyses by staining for PE-conjugated HPV16 E7aa49–57 peptide-loaded H-2 Db E7 tetramer and APC-A750-conjugated anti-mouse CD8α antibodies. Representative flow images of CD8+ and E7+ T cells for all 4 groups and (e) bar graph representations are shown. *p<0.05, **p<0.01, ***p<0.001, ****p<0.0001. S.C., subcutaneously; PBMC, peripheral blood mononuclear cells.
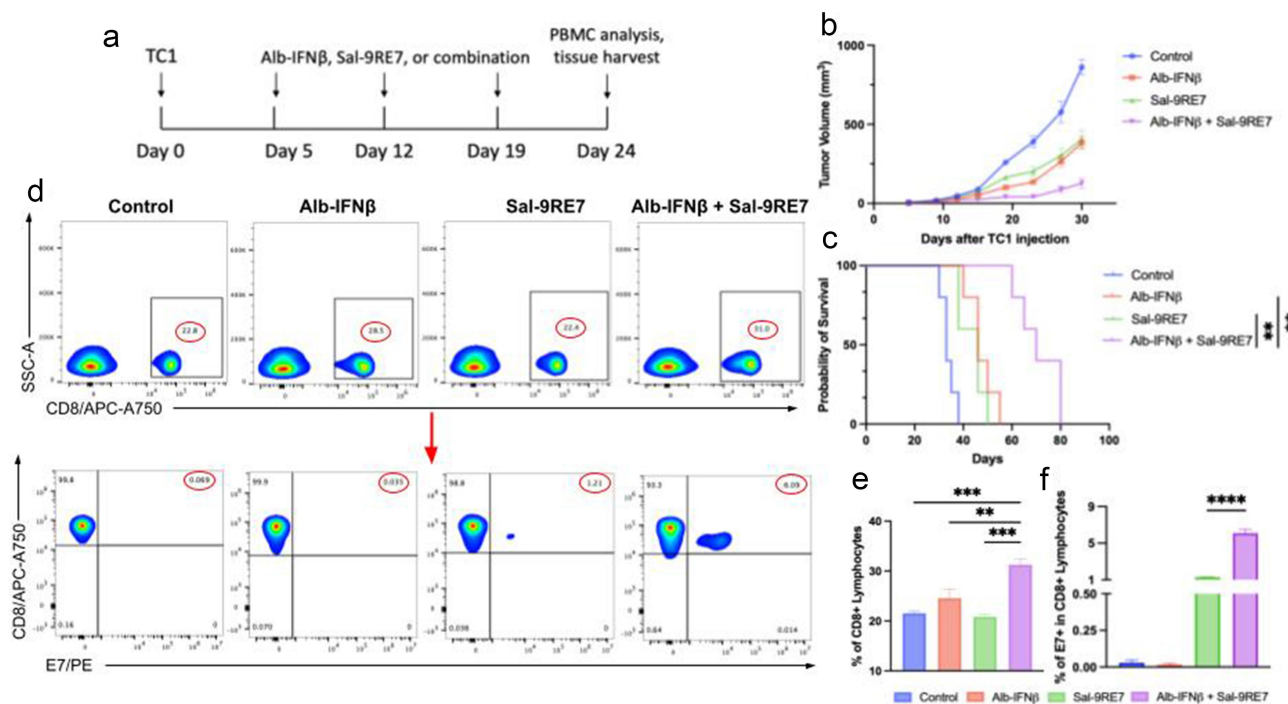

Figure 4. Characterization of antitumor effect and antigen specific CD8+ T cell response generated by Sal-9RE7 combined with adjuvant Alb-IFNβ. (a) Schematic illustration of the experiment. C57BL/6 mice were S.C. injected with 1×10^5 TC-1 cells. On day 5, they were given 50 ug Alb-IFNβ intraperitoneally, Sal-9RE7 (10^8 CFU to 10ug peptide) S.C., or combination treatment weekly for three times. PBMC tumors were harvested to analyze for tumor infiltrating lymphocytes. (b) Tumor growth curve of TC-1 tumor-bearing mice. (c) Kaplan-Meier survival curve of TC-1 tumor-bearing mice. (d) PBMC is stained for PE-conjugated HPV16 E7 tetramer and APC-A750-conjugated CD8α antibodies. Representative flow images and bar graphs showing (e) CD8+ T cell population and (f) E7+ subpopulation. **p<0.01, ***p<0.001, ****p<0.0001.

Alb-IFNβ with Sal-9RE7 (Figure 4a), tumor growths were suppressed at an earlier time point and achieved sustained control compared to individual treatments (Figure 4b). Additionally, the combination treatment effectively prolonged the median survival by 24 days than either individual treatment (Figure 4c). Significantly higher population of CD8+ T cells and E7-specific phenotypes (Figure 4d,e) were observed in the PBMC of Alb-IFNβ and Sal-9RE7 combination group compared to individual treatments. Thus, combining Alb-IFNβ and Sal-9RE7 enhanced antitumor effects and antigen-specific CD8+ T cell response.

Treatment with Alb-IFNβ and Sal-9RE7 increases CD4+ and CD8+ lymphocytes infiltration in the tumor microenvironment

Following treatment schedule (Figure 4a), TIL populations were analyzed with flow cytometry after the final treatment (Figure 5a). Under Sal-9RE7 treatment alone, the percentage of CD4+ T cells increased, but CD8+ population remained unchanged compared to the untreated group (Figure 5b). The opposite was observed in the Alb-IFNβ treated group, as only the CD8+ T cell population increased while CD4+ T cell population did not change (Figure 5c). By combining both treatments, both CD4+ and CD8+ T cell populations were elevated compared to the untreated control group. Upon examining CD8+ T cell exhaustion and regulatory T cell phenotypes (Figure 5d,f), the combination treatment yielded the least

amount of immune downregulation and exhaustion. Notably, combined treatment of Alb-IFNβ and Sal-9RE7 could significantly reverse the high PD-1 expression shown in the Sal-9RE7 treated group (Figure 5e) and decrease Treg phenotypes compared to the control group (Figure 5g). Thus, combining Alb-IFNβ and Sal-9RE7 simultaneously expanded CD4+ and CD8+ TIL populations while downregulated immune suppressing phenotypes.

Discussion

In this study, we have verified the strategy of displaying MHC class I tumor-associated epitope on bacterial surface to induce cancer immunity. Compared to live attenuated *Salmonella*, heat inactivated *Salmonella* had doubled the amount of peptide coated on its surface. This is because moderate heat stress on bacteria could induce cell permeabilization without cell lysis and structural damage,[25] allowing more peptide attachment and penetration of the bacterial outer membrane. In addition, modifications of the CPP by substituting the CPP anchor from 6K to 9 R further increased peptide adsorption by over 30-fold. This finding is consistent with a previous study that showed arginine-rich peptides promoted membrane permeabilization more than lysine.[26] With these engineering improvements, the antigen delivery platform has become more efficient and remained technically simple for scale-up production.

Although dead bacteria generate less immune response from granulocytes and macrophages compared to live
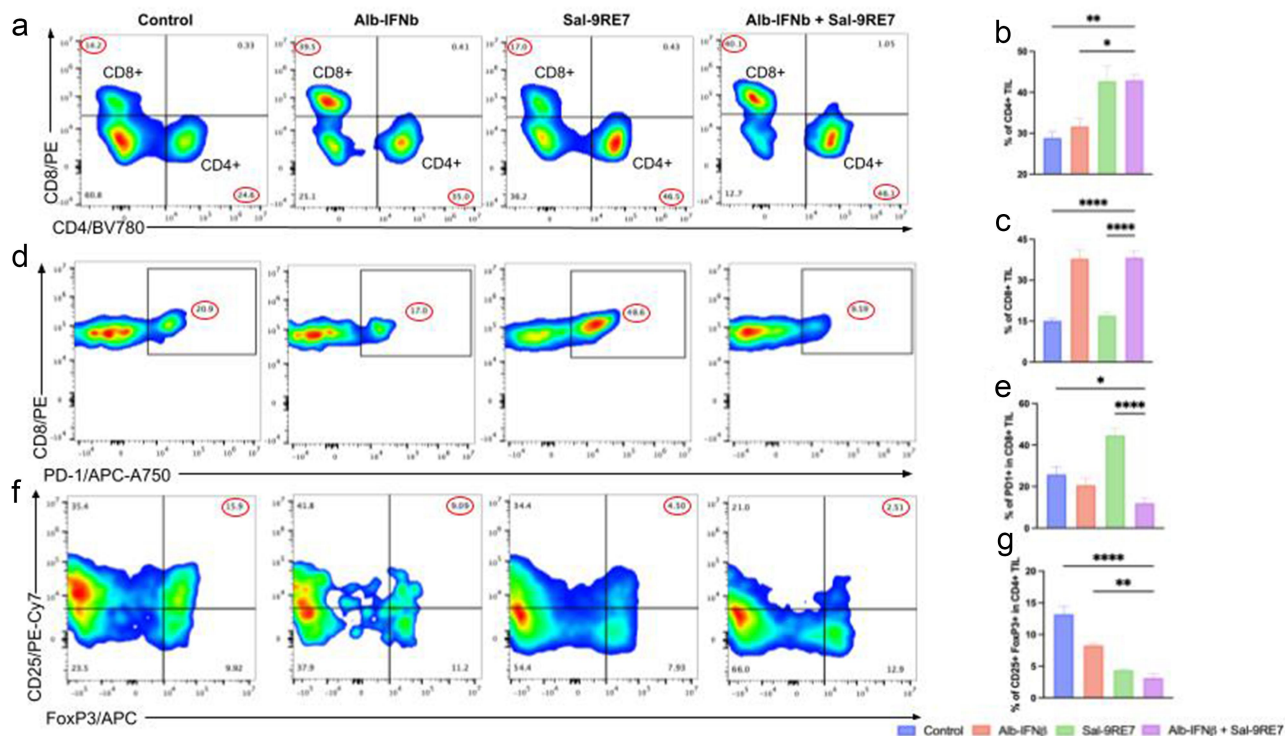

Figure 5. Characterization of CD4+ and CD8+ tumor infiltrating lymphocytes in Alb-IFNβ and Sal-9RE7 combination treatments. (a) Tumors from previously treated groups are extracted and isolated for mononuclear cells. TIL populations are identified by staining for PE-Cy5-conjugated anti-mouse CD45 and BV421-conjugated anti-mouse CD3 antibodies. Then PE-conjugated anti-mouse CD8 and BV780-conjugated anti-mouse CD4 antibodies are used to distinguish cytotoxic and helper T cell populations respectively. Representative flow cytometry gating strategy and bar graphs for (b) CD4+ and (c) CD8+ TILs are shown. (d) PD-1 expression on CD8+ TIL using APC-A750 conjugated anti-mouse PD-1 antibody staining, and (f) intratumoral Treg population with PE-Cy7-conjugated CD25 and APC-conjugated FoxP3 antibodies. Bar graph summary of (e) PD-1 expressing CD8+ TILs and (g) Treg population in CD4+ TILs. *p<0.05, **p<0.01, ****p<0.0001. TIL, tumor infiltrating lymphocytes; Treg, regulatory T cells.

bacteria,[27] we proved that they retained immunogenicity to activate APCs *in vitro*. The 9R moiety of the peptide did not affect E7 antigen processing and cross-presentation by APCs to activated antigen-specific CTLs. Peptide only group 9RE7 serves as a positive control for both dendritic cell uptake and T cell activation (Figure 2). The elevated IFNγ expression of 9RE7 treatment (Figure 2d) compared to the Sal-9RE7 is because peptide loaded dendritic cells present more efficiently than cross-presentation from protein.[28] Here, we observe the same phenomena as cross-presented antigen from Sal-9RE7 is less effective at activating E7-specific T cells than 9RE7 direct loading. But in mouse models, due to a lack of adjuvant accompanying 9RE7, the peptide alone cannot activate antigen-presenting cells to induce tumor antigen-specific immune response (Figure 3e).

In TC-1 tumor-bearing animal models, vaccination with Sal-9RE7 achieve significant antitumor control, while inducing E7-specific CTLs (Figure 3e). By injecting *Salmonella* subcutaneously, it allows a concentrated and sustained delivery that immunologically activated antigen presenting cells of the skin.[29] Initial bacterial injection attempts on the tumor-opposing side had limited the response rate and tumor control. After changing the injection to the tumor side, we observed better tumor control in the Sal-9RE7 treatment group. This can be due to *Salmonella* at the tumor-draining lymph node to target migratory dendritic cells and prime T cells for tumor infiltration,[30,31] while direct engagement of tumor draining lymph node that develops robust antitumor immunity.[32] Inflammation from the initial Sal-9RE7 dose cleared within days with little adverse effect on the mice. Tumor growth showed visible control after the third dose and achieved better antitumor effect and survival outcome than the previous BCG-OVA fusion construct, which was unable to control B16.OVA tumor growth as a monotherapy.[12] Aside from using a different tumor model, our results could be due to the improved antigen delivery system Sal-9RE7 and higher permissible dose by inactivating *Salmonella* via heat shock, which led to more robust E7-specific T cells immunity. In terms of other possible injection routes, this treatment could benefit from intratumoral delivery, which could possibly induce an earlier onset of tumor control by priming E7-specific TILs in solid tumors.[33]

Current bacterial therapy methods have combined bacterial treatment with traditional therapies for enhanced immunogenicity and specific tumor cell targeting.[13,34,35] Here, we paired Sal-9RE7 with the novel protein-based adjuvant Alb-IFNβ. We observed slightly elevated peripheral CD8+ T cells in the Alb-IFNβ group compared to Sal-9RE7, while the combination treatment of Alb-IFNβ and Sal-9RE7 significantly expanded CD8+ T cells and E7 antigen-specific CD8 + T cells. This is because type I interferons could increase antigen presentation by APCs and costimulatory factors in T cell activation.[36] In addition, the flow cytometry analysis of the TME showed Alb-IFNβ solely acted on increasing CD8+ T cells population (Figure 5c), while Sal-9RE7 only increased CD4+ TILs (Figure 5b). By combining the two treatments, both CD8+ and CD4+ T cell populations were elevated and induced a more robust antitumor immunity. This is because intratumoral CD4+ helper T cells can increase immune

function and population of tumor-specific CD8+ T cells through IL-2 production.[37] In addition, Sal-9RE7 monotherapy exhibited high T cell exhaustion in the expression of PD-1, but this was reduced by combining with Alb-IFNβ because type I interferon has been shown to downregulate Tregs and promote effector cell functions.[16] The decreased immune exhaustion in the TME can explain the significant improvement in antitumor efficacy with the combination therapy. Overall, these results show that the antigen-coated bacterial vaccine, Sal-9RE7, can benefit from combined treatment with Alb-IFNβ.

In terms of mechanism of therapy, bacterial immunity engages antigen-presenting cells, the complement system, and adaptive immunity. For *Salmonella*, studies suggest that CD4+ T cells play a central role in developing protective immunity.[38–40] We observed that Sal-9RE7 treatment recruits CD4+ T cells to the TME (Figure 5b), confirming that CD4+ T cells respond to *Salmonella* infection. But without E7 coating, *Salmonella* alone could not induce any antitumor response (Figure 3b) because no tumor-specific cytotoxic T cells were present (Figure 3e). So despite CD8+ TIL population not increasing in response to Sal-9RE7 treatment (Figure 5c), having developing E7 antigen specificity from dendritic cells cross-presentation is critical for antitumor immunity. When the adjuvant cytokine Alb-IFNβ is introduced as a combination therapy to Sal-9RE7, it engaged CTL prolifferation that lacked in Sal-9RE7. Previously, we saw that type I infeteron can promote antigen-specific CD8+ T cell infiltration in the TME through CXCL-9 and CXCL-10 proliferation.[20,41] While the combination treatment's intended antitumor mechanism is to engage antigen-specific T cells, other mechanisms could play a role as well and should be investigated further for a more comprehensive understanding of this strategy.

Thus, we have demonstrated the therapeutic efficacy of the tumor antigen-presenting bacterial vaccine Sal-9RE7 and improvements on synthesis efficiency to induce more robust tumor-specific immune responses. Significant enhancement in antitumor effect was achieved through pairing Sal-9RE7 with protein adjuvant Alb-IFNβ. This demonstrates the potential of bacterial immunotherapy in conjunction with other cancer therapies to achieve superior treatment results. Future investigations of peptide-coated bacterial vaccines should expand the tumor MHC class I epitope library to explore its efficacy and applicability in other cancer cell types. For more potent antitumor effect, neoantigen-coated bacteria should be combined with established cancer therapies inducing chemotherapy, radiation, and immunotherapy strategies to increase treatment response rate. Further investigation in comparing the efficacy and safety of live attenuated versus dead bacteria should be explored, in order to address safety and treatment response limitations by providing more effective and personalized cancer therapy.

Disclosure statement

Funding

Availability of data and material

All data relevant to the study are included in the article or uploaded as supplementary information. Data and materials are available on reasonable request.

Authors' contributions

Conception and design: S.W., CF.H.
Conducting experiments: S.W., CC.C., YC.T.
Analysis and interpretation of data: S.W., CY.C., YC.T. JM.Y.
Writing and review of manuscript: S.W., M.C., CF.H.
Study supervision: T.C. W, CH.H., CF.H.

References

1. Gupta KH, Nowicki C, Giurini EF, Marzo AL, Zloza A. Bacterial-based cancer therapy (BBCT): recent advances, Current challenges, and future prospects for cancer immunotherapy. Vaccines (Basel). 2021;9(12):1497. doi: 10.3390/vaccines9121497.

2. Liang S, Wang C, Shao Y, Wang Y, Xing D, Geng Z. Recent advances in bacteria-mediated cancer therapy. Front Bioeng Biotechnol. 2022;10:1026248. doi: 10.3389/fbioe.2022.1026248.

3. Phan TX, Nguyen VH, Duong MT, Hong Y, Choy HE, Min JJ. Activation of inflammasome by attenuated salmonella typhimurium in bacteria-mediated cancer therapy. Microbiol Immunol. 2015;59(11):664–75. doi: 10.1111/1348-0421.12333.

4. Xiao S, Shi H, Zhang Y, Fan Y, Wang L, Xiang L, Liu Y, Zhao L, Fu S. Bacteria-driven hypoxia targeting delivery of chemotherapeutic drug proving outcome of breast cancer. J Nanobiotechnology. 2022;20(1):178. doi: 10.1186/s12951-022-01373-1.

5. Yu B, Yang M, Shi L, Yao Y, Jiang Q, Li X, Tang L-H, Zheng B-J, Yuen K-Y, Smith DK, et al. Explicit hypoxia targeting with tumor suppression by creating an "obligate" anaerobic salmonella typhimurium strain. Sci Rep. 2012;2(1):436. doi: 10.1038/srep00436.

6. Gurbatri CR, Arpaia N, Danino T. Engineering bacteria as interactive cancer therapies. Sci. 2022;378(6622):858–64. doi: 10.1126/science.add9667.

7. Chandra D, Selvanesan BC, Yuan Z, Libutti SK, Koba W, Beck A, Zhu K, Casadevall A, Dadachova E, Gravekamp C, et al. 32-phosphorus selectively delivered by listeria to pancreatic cancer demonstrates a strong therapeutic effect. Oncotarget. 2017;8(13):20729–40. doi: 10.18632/oncotarget.15117.

8. Aganja RP, Sivasankar C, Senevirathne A, Lee JH. Salmonella as a promising curative tool against cancer. Pharmaceutics. 2022;14(10):2100. doi: 10.3390/pharmaceutics14102100.

9. Al-Ramadi BK, Fernandez-Cabezudo MJ, El-Hasasna H, Al-Salam S, Bashir G, Chouaib S. Potent anti-tumor activity of systemically-administered IL2-expressing salmonella correlates with decreased angiogenesis and enhanced tumor apoptosis. Clin Immunol. 2009;130(1):89–97. doi: 10.1016/j.clim.2008.08.021.

10. Kung YJ, Lam B, Tseng SH, MacDonald A, Tu HF, Wang S, Lin J, Tsai YC, Wu TC, Hung C-F, et al. Localization of Salmonella and albumin-IL-2 to the tumor microenvironment augments anticancer T cell immunity. J Biomed Sci. 2022;29(1):57. doi: 10.1186/s12929-022-00841-y.

11. Nishikawa H, Sato E, Briones G, Chen LM, Matsuo M, Nagata Y, et al. In vivo antigen delivery by a Salmonella typhimurium type III secretion system for therapeutic cancer vaccines. J Clin Invest. 2006;116(7):1946–1954. doi: 10.1172/JCI28045.

12. Ylösmäki E, Fusciello M, Martins B, Feola S, Hamdan F, Chiaro J, Ylösmäki L, Vaughan MJ, Viitala T, Kulkarni PS, et al. Novel personalized cancer vaccine platform based on Bacillus Calmette-Guèrin. J Immunother Cancer. 2021;9(7):e002707. doi: 10.1136/jitc-2021-002707.

13. Bayat Mokhtari R, Homayouni TS, Baluch N, Morgatskaya E, Kumar S, Das B, Yeger H. Combination therapy in combating cancer. Oncotarget. 2017;8(23):38022–38043. doi: 10.18632/oncotarget.16723.

14. Dunn GP, Old LJ, Schreiber RD. The immunobiology of cancer immunosurveillance and immunoediting. Immunity. 2004;21(2):137–48. doi: 10.1016/j.immuni.2004.07.017.

15. Guillot B, Portalès P, Thanh AD, Merlet S, Dereure O, Clot J, Corbeau P. The expression of cytotoxic mediators is altered in mononuclear cells of patients with melanoma and increased by interferon-alpha treatment. Br J Dermatol. 2005;152(4):690–696. doi: 10.1111/j.1365-2133.2005.06512.x.

16. Zitvogel L, Galluzzi L, Kepp O, Smyth MJ, Kroemer G. Type I interferons in anticancer immunity. Nat Rev Immunol. 2015;15(7):405–14. doi: 10.1038/nri3845.

17. Tarhini AA, Cherian J, Moschos SJ, Tawbi HA, Shuai Y, Gooding WE, Sander C, Kirkwood JM. Safety and efficacy of combination immunotherapy with interferon alfa-2b and tremelimumab in patients with stage IV melanoma. J Clin Oncol. 2012;30(3):322–328. doi: 10.1200/JCO.2011.37.5394.

18. Preudhomme C, Guilhot J, Nicolini FE, Guerci-Bresler A, Rigal-Huguet F, Maloisel F, Coiteux V, Gardembas M, Berthou C, Vekhoff A, et al. Imatinib plus peginterferon alfa-2a in chronic myeloid leukemia. N Engl J Med. 2010;363(26):2511–21. doi: 10.1056/NEJMoa1004095.

19. Burchert A, Müller MC, Kostrewa P, Erben P, Bostel T, Liebler S, Hehlmann R, Neubauer A, Hochhaus A. Sustained molecular response with interferon alfa maintenance after induction therapy with imatinib plus interferon alfa in patients with chronic myeloid leukemia. J Clin Oncol. 2010;28(8):1429–1435. doi: 10.1200/JCO.2009.25.5075.

20. Tseng SH, Cheng MA, Farmer E, Ferrall L, Kung YJ, Lam B, Lim L, Wu T-C, Hung C-F. Albumin and interferon-β fusion protein serves as an effective vaccine adjuvant to enhance antigen-specific CD8+ T cell-mediated antitumor immunity. J Immunother Cancer. 2022;10(4):e004342. doi: 10.1136/jitc-2021-004342.

21. Cutrona KJ, Kaufman BA, Figueroa DM, Elmore DE. Role of arginine and lysine in the antimicrobial mechanism of histone-derived antimicrobial peptides. FEBS Lett. 2015;589(24PartB):3915–20. doi: 10.1016/j.febslet.2015.11.002.

22. Wang TL, Ling M, Shih IM, Pham T, Pai SI, Lu Z, Kurman RJ, Pardoll DM, Wu T-C. Intramuscular administration of E7-transfected dendritic cells generates the most potent E7-specific anti-tumor immunity. Gene Ther. 2000;7(9):726–733. doi: 10.1038/sj.gt.3301160.

23. Shen Z, Reznikoff G, Dranoff G, Rock KL. Cloned dendritic cells can present exogenous antigens on both MHC class I and class II molecules. J Immunol. 1997;158(6):2723–30. doi: 10.4049/jimmunol.158.6.2723.

24. Ma Y, Yang A, Peng S, Qiu J, Farmer E, Hung CF, Wu T-C. Characterization of HPV18 E6-specific T cell responses and establishment of HPV18 E6-expressing tumor model. Vaccine. 2017;35(31):3850–3858. doi: 10.1016/j.vaccine.2017.05.081.

25. Ebrahimi A, Csonka LN, Alam MA. Analyzing thermal stability of cell membrane of salmonella using time-multiplexed impedance sensing. Biophys J. 2018;114(3):609–18. doi: 10.1016/j.bpj.2017.10.032.

26. Fuchs SM, Raines RT. Polyarginine as a multifunctional fusion tag. Protein Sci. 2005;14(6):1538–44. doi: 10.1110/ps.051393805.

27. Lentini G, De Gaetano GV, Famà A, Galbo R, Coppolino F, Mancuso G, Teti G, Beninati C. Neutrophils discriminate live from dead bacteria by integrating signals initiated by Fprs and TLRs. EMBO J. 2022;41(5):e109386. doi: 10.15252/embj.2021109386.

28. Met O, Buus S, Claesson MH. Peptide-loaded dendritic cells prime and activate MHC-class I-restricted T cells more efficiently than protein-loaded cross-presenting DC. Cellular Immunology. 2003;222(2):126–133. doi: 10.1016/S0008-8749(03)00128-X.

29. Romani N, Flacher V, Tripp CH, Sparber F, Ebner S, Stoitzner P. Targeting skin dendritic cells to improve intradermal vaccination. Curr Top Microbiol Immunol. 2012;351:113–138.

30. van Pul KM, Fransen MF, van de Ven R, de Gruijl TD, van Pul KM. Immunotherapy goes local: the central role of lymph nodes in driving tumor infiltration and efficacy. Front Immunol. 2021;12:643291. doi: 10.3389/fimmu.2021.643291.

31. Marion Pitorre GB, Bastiat G, Dit Chatel EM, Benoit J-P. Elodie Marie dit Chatel, Jean-Pierre Benoit. Passive and specific targeting of lymph nodes: the influence of the administration route. Eur J Nanomed. 2015;7(2). doi: 10.1515/ejnm-2015-0003.

32. Koukourakis MI, Giatromanolaki A. Tumor draining lymph nodes, immune response, and radiotherapy: towards a revisal of therapeutic principles. Biochim Biophys Acta Rev Cancer. 2022;1877(3):188704. doi: 10.1016/j.bbcan.2022.188704.

33. Hong WX, Haebe S, Lee AS, Westphalen CB, Norton JA, Jiang W, Levy R. Intratumoral immunotherapy for early-stage solid tumors. Clin Cancer Res. 2020;26(13):3091–3099. doi: 10.1158/1078-0432.CCR-19-3642.

34. Wu W, Pu Y, Gao S, Shen Y, Zhou M, Yao H, Shi J. Bacterial metabolism-initiated nanocatalytic tumor immunotherapy. Nanomicro Lett. 2022;14(1):220. doi: 10.1007/s40820-022-00951-0.

35. Yi X, Zhou H, Chao Y, Xiong S, Zhong J, Chai Z, Yang K, Liu Z. Bacteria-triggered tumor-specific thrombosis to enable potent photothermal immunotherapy of cancer. Sci Adv. 2020;6(33): eaba3546. doi: 10.1126/sciadv.aba3546.

36. Welsh RM, Bahl K, Marshall HD, Urban SL, Rall GF. Type 1 interferons and antiviral CD8 T-cell responses. PLoS Pathog. 2012;8(1):e1002352. doi: 10.1371/journal.ppat.1002352.

37. McSorley SJ, Cookson BT, Jenkins MK. Characterization of CD4+ T cell responses during natural infection with salmonella typhimurium. J Immunol. 2000;164(2):986–93. doi: 10.4049/jimmunol.164.2.986.

38. Antonelli AC, Binyamin A, Hohl TM, Glickman MS, Redelman-Sidi G. Bacterial immunotherapy for cancer induces CD4-dependent tumor-specific immunity through tumor-intrinsic interferon-γ signaling. Proc Natl Acad Sci U S A. 2020;117 (31):18627–37. doi: 10.1073/pnas.2004421117.

39. Hess J, Ladel C, Miko D, Kaufmann SH. Salmonella typhimurium aroA- infection in gene-targeted immunodeficient mice: major role of CD4+ TCR-alpha beta cells and IFN-gamma in bacterial clearance independent of intracellular location. J Immunol. 1996;156 (9):3321–6. doi: 10.4049/jimmunol.156.9.3321.

40. Ravindran R, McSorley SJ. Tracking the dynamics of T-cell activation in response to Salmonella infection. Immunology. 2005;114 (4):450–8. doi: 10.1111/j.1365-2567.2005.02140.x.

41. Cao X, Liang Y, Hu Z, Li H, Yang J, Hsu EJ, Zhu J, Zhou J, Fu Y-X. Next generation of tumor-activating type I IFN enhances anti-tumor immune responses to overcome therapy resistance. Nat Commun. 2021;12(1):5866. doi: 10.1038/s41467-021-26112-2.